Electronic Supplementary Material (ESI) for Materials Advances.

Supporting Information

Porous Organic Polymer-Coated Permselective Separator Mitigating Self- Discharge for Lithium-Sulfur Batteries

Deepa Elizabeth Mathew[a,b], Sivalingam Gopi[a,b], Murugavel Kathiresan[a,b]*, G. Jenita Rani[c], Sabu Thomas[d], A Manuel Stephan[a,b]*

[a] *CSIR- Central Electrochemical Research Institute, Karaikudi 630 003, India.*

[b] *Academy of Scientific and Innovative Research (AcSIR), CSIR-CECRI Campus, Karaikudi, India*

[c] *Department of Physics, Fatima College (Autonomous), Madurai 625 017, India*

[d] *International and Inter-University Centre for Nanoscience and Nanotechnology, Mahatma Gandhi University, Kottayam, 686560, India.*

*Corresponding authors
Tel: +91 4565 241426 Fax: +91 4565 27779
e-mail: amstephan@cecri.res.in
kathiresan@cecri.res.in

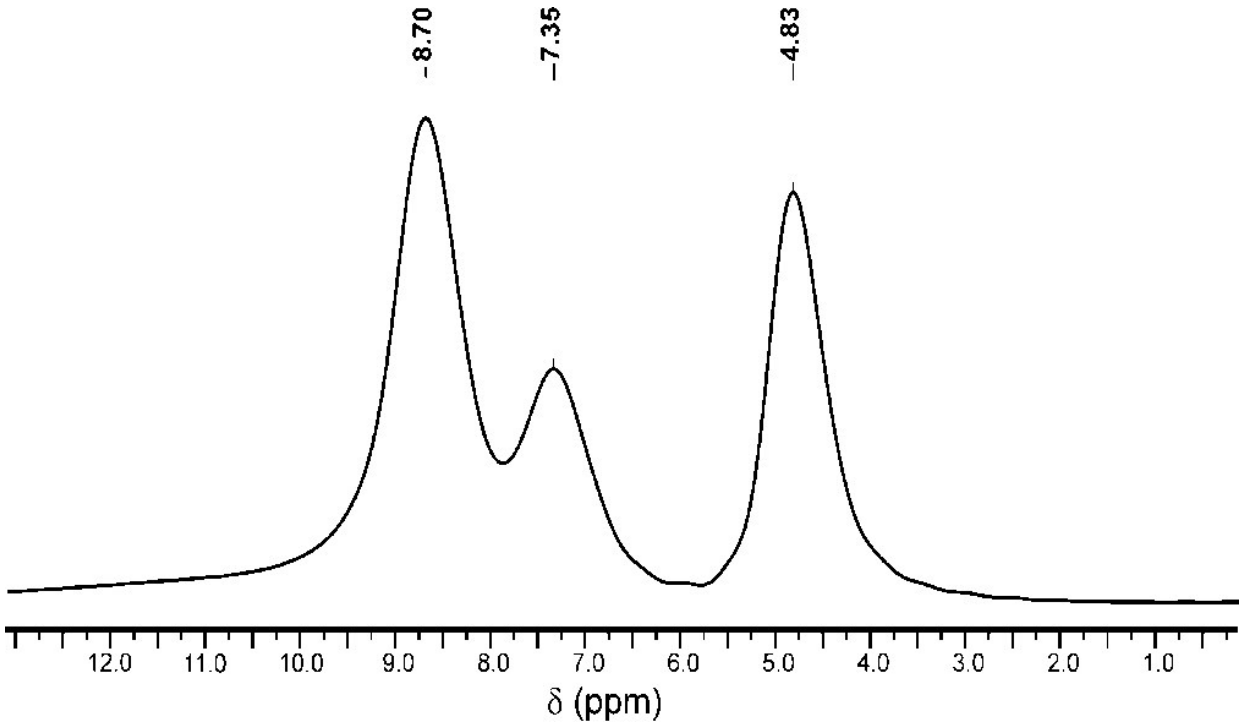

Figure S1 a. Solid-state ^{1}H NMR of TP-POP

The aromatic phenylene groups of the POP were observed at δ 8.70 ppm, whereas the terminal groups of the POP were observed at δ 7.35 ppm with low intensity. A slight upfield shift in the terminal protons indicates that these groups belong to phenylenediamine with NH_2 terminals. 'NH' group of phenylene diamine interconnection was observed at δ 4.83 ppm.

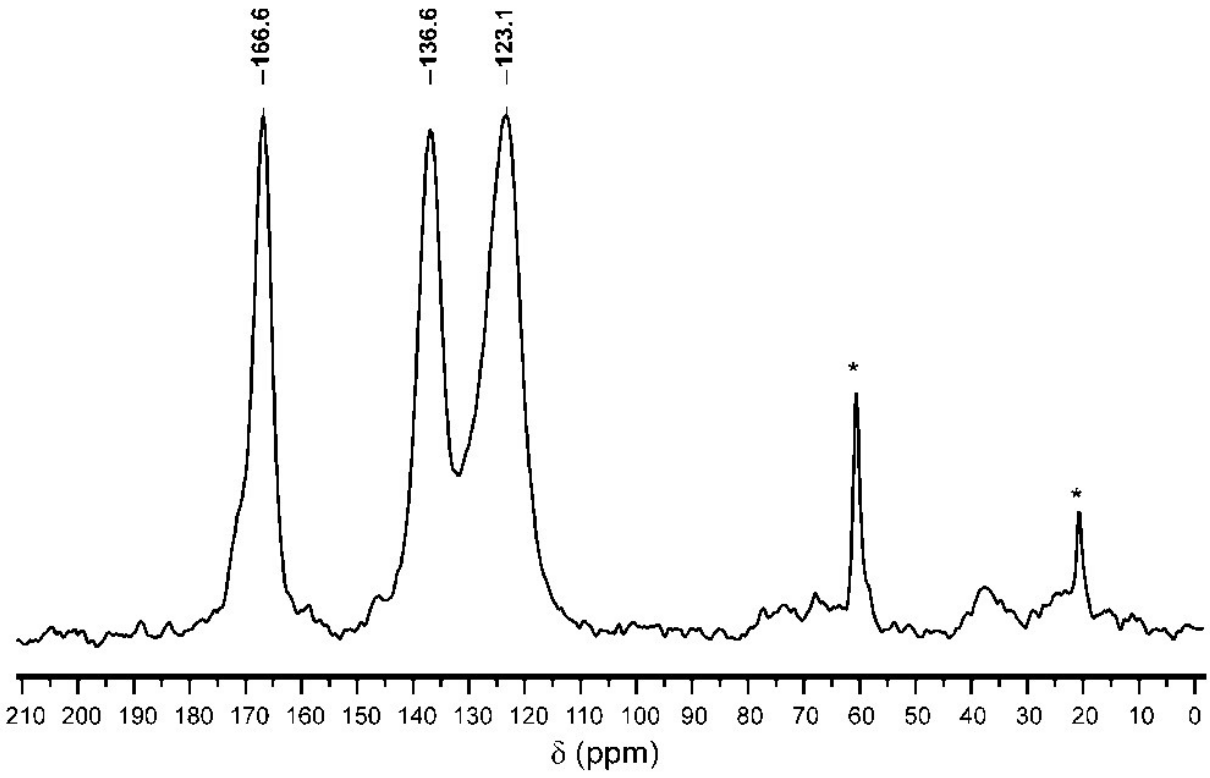

Figure S1 b. Solid-state ^{13}C NMR of TP-POP

^{13}C CP-MAS solid-state NMR of the **TP-POP** sample showed three peaks at 166.6, 136.6, and 123.1 ppm and are ascribed to three sp^2 carbons of the POP sample. The tertiary triazine carbons were observed at δ 166.6 ppm due to the electron-withdrawing effect of triazine 'N' groups. Similarly, the tertiary carbon attached to NH nitrogen of phenylene diamine was observed at δ 136.6 ppm. The phenylene group carbon was observed at δ 123.1 ppm. It is noteworthy that we did not observe any residual cyanuric chloride or 1,4-phenylene diamine carbon peaks which is an indication of completion of polymerization between cyanuric chloride and 1,4-phenylenediamine.[1]

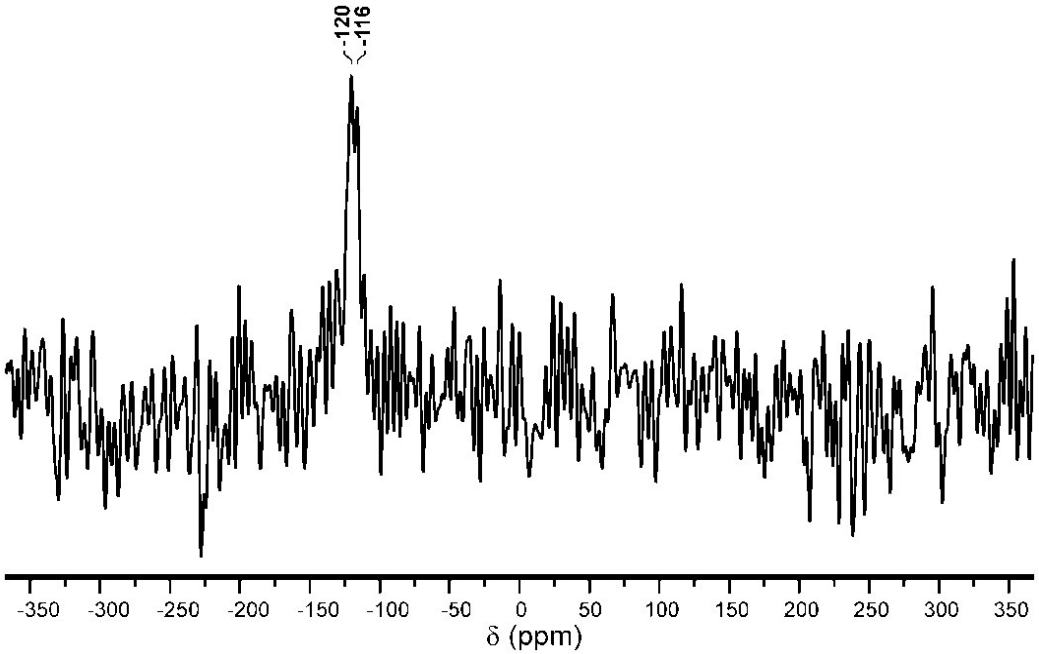

Figure S1 c. Solid-state ^{15}N NMR of TP-POP

Solid-state ^{15}N NMR confirmed the presence of two different nitrogen atoms present in the sample, i.e., triazine 'N' atδ -120.3 ppm and 'NH' of the 1,4-phenylenediamine at δ -116.2 ppm.[1]

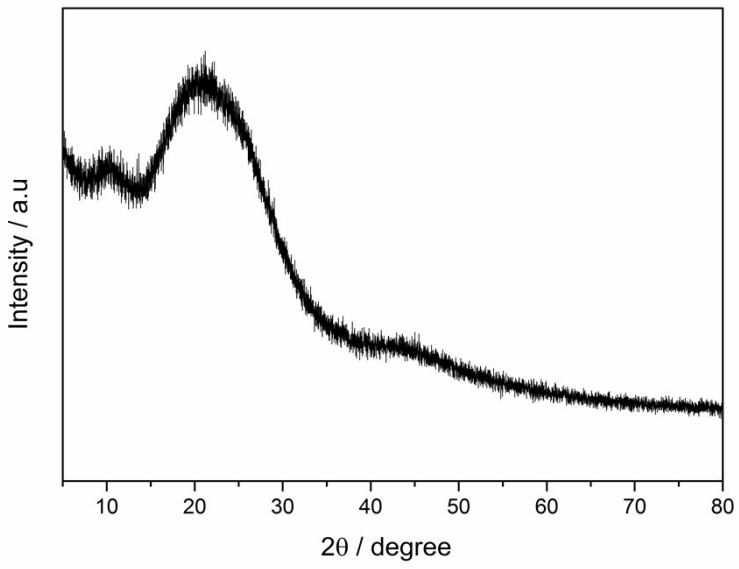

Figure S1 d. Powder XRD analysis of the TP-POP.

The powder X-ray analysis of the TP-POP sample revealed its amorphous nature with a 2θ value of 21.2 degrees (Figure S4). The broad diffraction peak in this range indicates the stacking of layered conjugated aromatic systems[1].

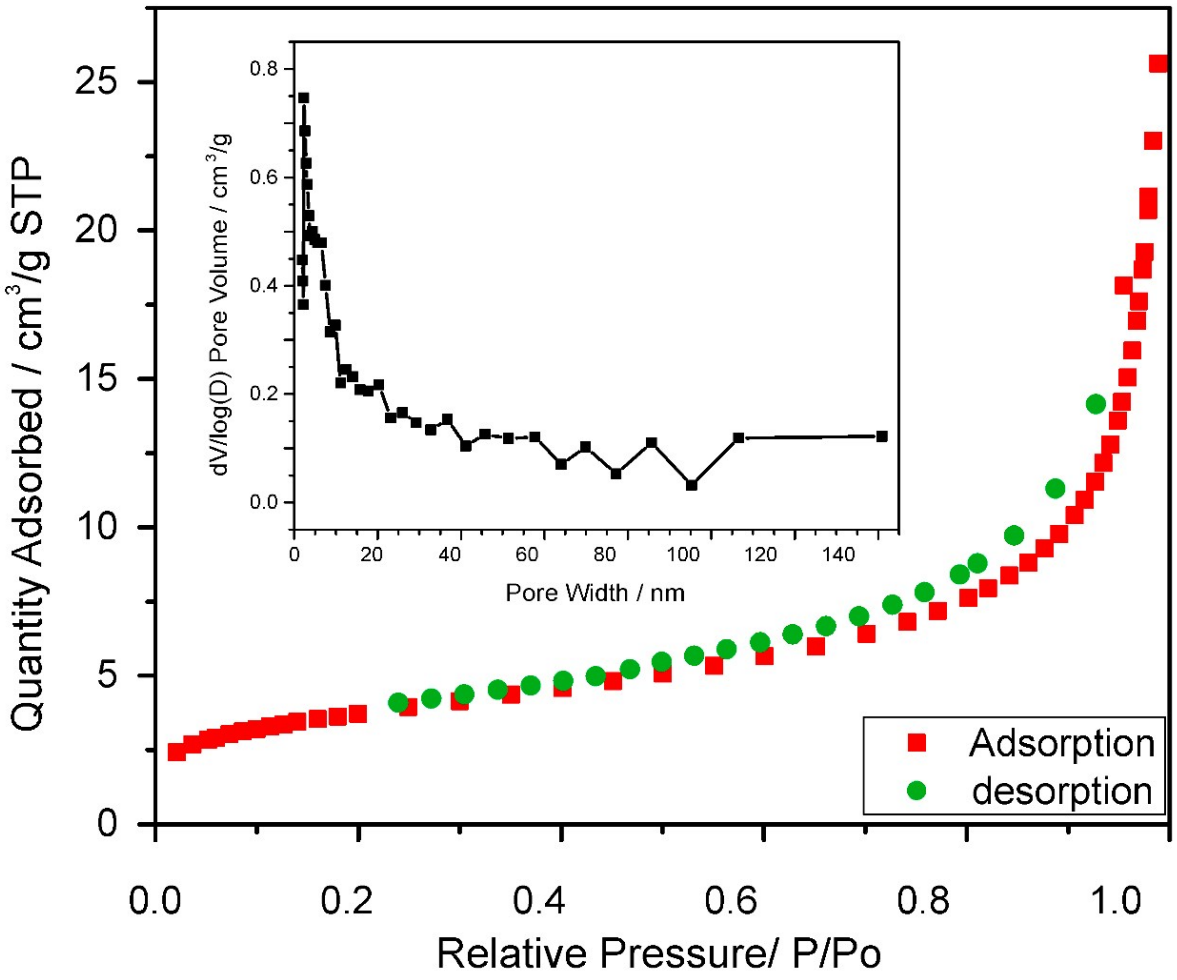

Figure S1 e. BET surface area analysis of porous organic polymer

The porous nature of the sample was determined by measuring N_2 adsorption-desorption analysis at 77 K. The sample represents type III isotherm with a BET surface area of 34 m^2/g. The pore dimension indicates that the sample contains a large fraction of mesopores and a smaller fraction of macropores. Single point adsorption total pore volume of pores less than 1802.130 Å diameter at P/Po = 0.989153172: 0.039637 $cm^3\ g^{-1}$. The adsorption average pore width (4V/A by BET) and BJH Desorption average pore diameter (4V/A) was respectively measured as 120.0 Å and 142.0 Å.

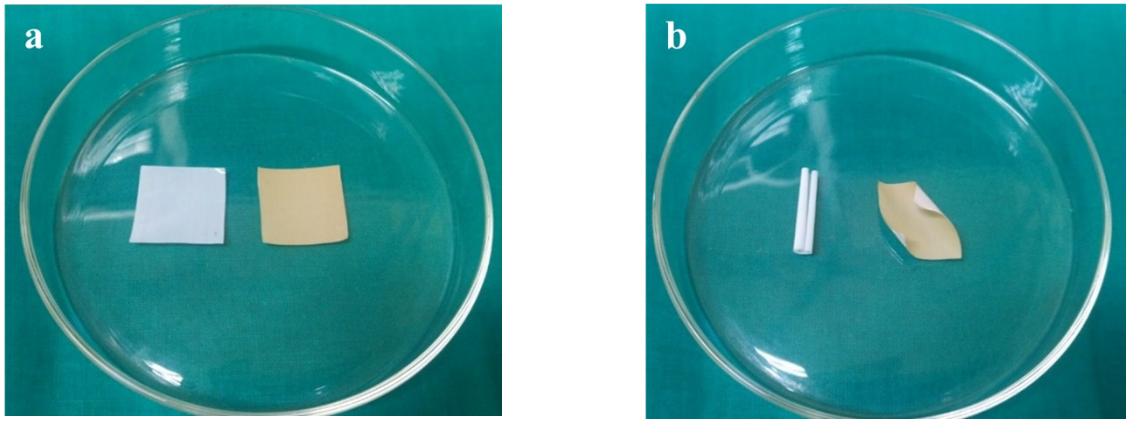

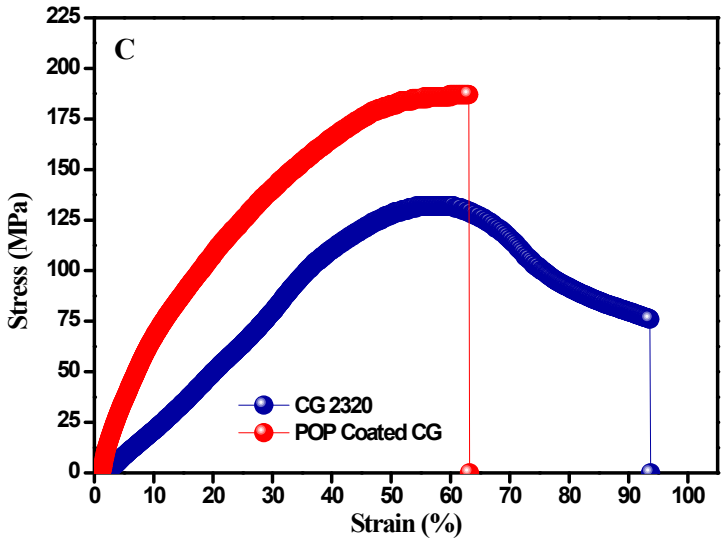

Sample	Elongation at break (%)	Maximum Tensile Strength (MPa)	Stress at break (MPa)
CG 2320	93	132	76
POP- CG	63	187	186.9

Figure S2. Digital photographs of a) Celgard 2320 and POP coated CG before heating b) after heating for 1 hour at 120 ℃ and c) Tensile stress–strain plots of CG 2320 and POP coated CG.

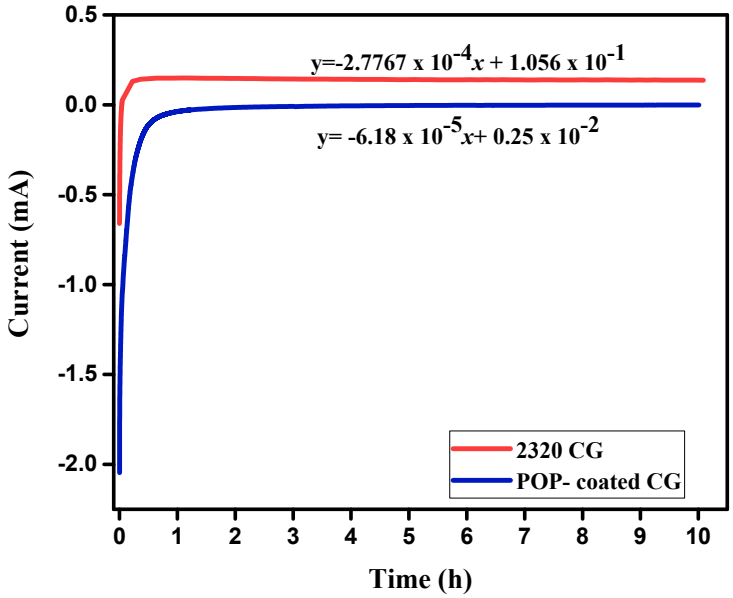

Figure S3. The current profile of the cell with Celgard 2320 and POP- coated CG held at a constant potential of 2.3 V.

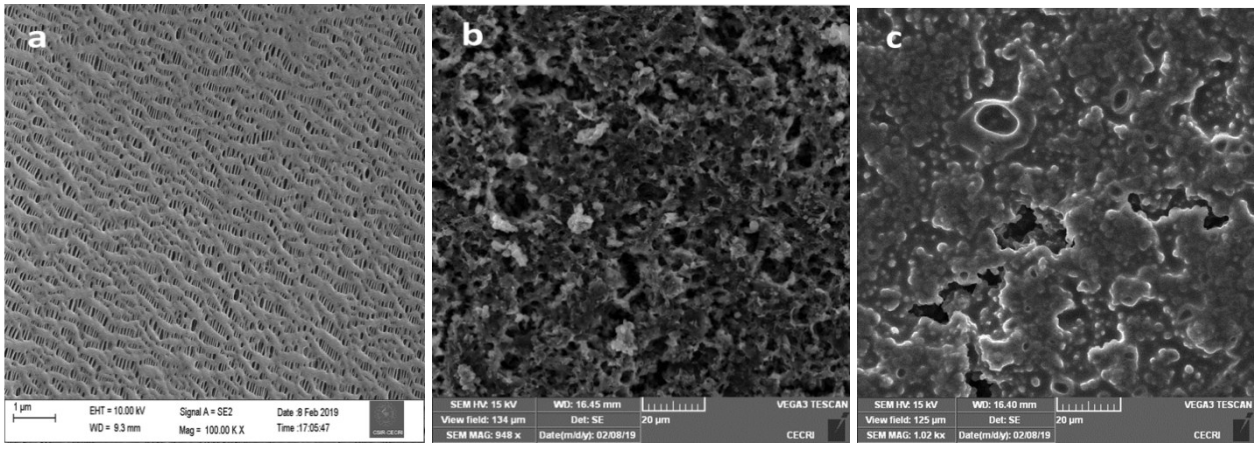

Figure S4. SEM images of (a) CG 2320 (b) POP - CG separator before cycling (c) after cycling.

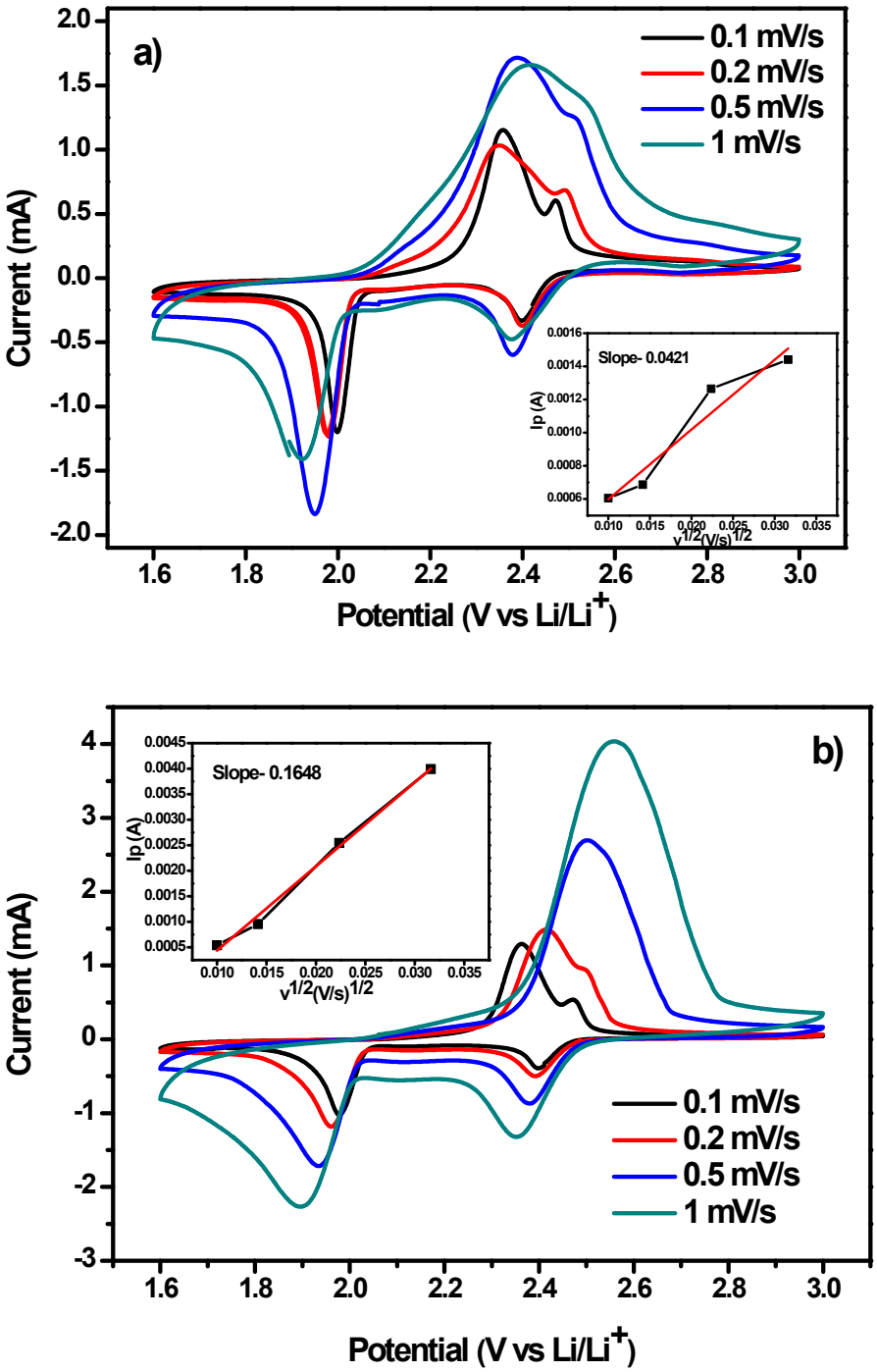

Figure S5. Cyclic voltammograms of Li S cell with a) CG 2320 b) POP- CG at different scanning rates

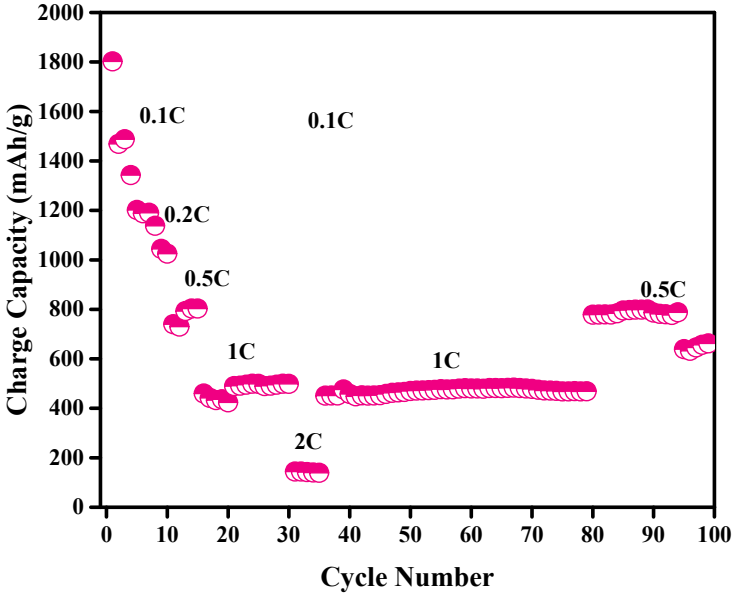

Figure S6. The charging capacity vs. Cycle number of Li-S cell with POP-coated Celgard

Table 1. Comparison of electrochemical properties of Li S cells with different permselective separators

Sl. No	Coating material	Thickness (µm)	Sulfur content in electrode	Initial capacity (mAh g^{-1})	Coulombic efficiency (%)	Capacity decay per cycle	Reference
1.	POP	7.17	2.47mg cm^{-2}	1390	90	-	This work
2.	Montmorillonite (MMT)	25	80 wt%	1380	97	NA	[2]
3.	Sulfonated acetylene black	6	72wt%	1262	95	NA	[3]
4.	$Cu_3(BTC)_2$ (HKUST-1) MOF@GO	NA	0.6-0.8 mg cm^{-2}	1207	98	0.019% (1 C)	[4]
5.	V_2O_5-decorated CNF	NA	2 mg cm^{-2}	1432	97	0.03% (3 C)	[5]
6.	CNT OH	NA	3 mg cm^{-2}	1056 (0.5C)	97	0.11% (0.5 C)	[6]
7.	Organically modified CNT	NA	50 wt%	1179	98	0.1% (2 C)	[7]
8.	Mn-BTC MOF	25	65wt%	1430	94	NA	[8]
9.	UiO-66-NH_2@SiO_2	55–60	72 wt%	1400	94	NA	[9]
10.	MWCNT/N-doped carbon quantum dot	NA	1.3–1.5 mg cm^{-2}	1330.8	96	0.05% (0.5 C)	[10]
11.	laponite nanosheets/ carbon black	3.5	1.0–1.2 mg cm^{-2}	1387	98	0.06% (0.2 C)	[11]
12.	$Ni_3(HITP)_2$	NA	70wt%	1403	99	0.032% (1 C)	[12]
13.	RAPOP/AB-PP	10	3- 3.5 mg cm^{-2}	1346 ($mAcm^{-2}$)	99	NA	[13]
14.	DMTA-COF	NA	0.6 mg cm^{-2}	1415 (0.5 C)	99.5	0.24% (0.5 C)	[14]
15.	CNT/ZrO_2	14	1.5 mg cm^{-2}	1207	95	NA	[15]
16.	TiO_2NS/CNT	10	0.86 mg cm^{-2}	1247 (0.2 C)	98	NA	[16]

References

1 S. Gopi and M. Kathiresan, *Polymer (Guildf).*, 2017, **109**, 315–320.

2 W. Ahn, S. N. Lim, D. U. Lee, K. B. Kim, Z. Chen and S. H. Yeon, *J. Mater. Chem. A*, 2015, **3**, 9461–9467.

3 F. Zeng, Z. Jin, K. Yuan, S. Liu, X. Cheng, A. Wang, W. Wang and Y. S. Yang, *J. Mater. Chem. A*, 2016, **4**, 12319–12327.

4 S. Bai, X. Liu, K. Zhu, S. Wu and H. Zhou, *Nat. Energy*, 2016, **1**, 16094.

5 M. Liu, Q. Li, X. Qin, G. Liang, W. Han, D. Zhou, Y. B. He, B. Li and F. Kang, *Small*, 2017, **13**, 1–7.

6 R. Ponraj, A. G. Kannan, J. H. Ahn, J. H. Lee, J. Kang, B. Han and D. W. Kim, *ACS Appl. Mater. Interfaces*, 2017, **9**, 38445–38454.

7 B. Liu, X. Wu, S. Wang, Z. Tang, Q. Yang, G. H. Hu and C. Xiong, *Nanomaterials*, 2017, **7**, 196.

8 S. Suriyakumar, M. Kanagaraj, M. Kathiresan, N. Angulakshmi, S. Thomas and A. M. Stephan, *Electrochim. Acta*, 2018, **265**, 151–159.

9 S. Suriyakumar, A. M. Stephan, N. Angulakshmi, M. H. Hassan and M. H. Alkordi, *J. Mater. Chem. A*, 2018, **6**, 14623–14632.

10 Y. Pang, J. Wei, Y. Wang and Y. Xia, *Adv. Energy Mater.*, 2018, **8**, 1–11.

11 Y. Yang and J. Zhang, *Adv. Energy Mater.*, 2018, **8**, 1–9.

12 Y. Zang, F. Pei, J. Huang, Z. Fu, G. Xu and X. Fang, *Adv. Energy Mater.*, 2018, **8**, 1–9.

13 Z. Wang and S. Wang, *Electrochim. Acta*, 2019, **306**, 229–237.

14 J. Wang, L. Si, Q. Wei, X. Hong, S. Cai and Y. Cai, *ACS Appl. Nano Mater.*, 2017, **1**, 132–138.

15 B. Liu, S. Wang, X. Wu, Z. Liu, Z. Gao, C. Li, Q. Yang, G. H. Hu and C. Xiong, *AIP Adv.*, 2018, **8**, 1–10.

16 P. Chen, Z. Wang, B. Zhang, J. Zhao, H. Liu, X. Guo, W. Liu and Z. Su, *Int. J. Energy Res.*, 2020, **44**, 3231–3240.